Retinex Preprocessing for Improved Multi-spectral Image Classification

B. Thompson, Z. Rahman, and S. Park

College of William & Mary, Department of Computer Science, Williamsburg, VA 23187

ABSTRACT

The goal of multi-image classification is to identify and label "similar regions" within a scene. The ability to correctly classify a remotely sensed multi-image of a scene is affected by the ability of the classification process to adequately compensate for the effects of atmospheric variations and sensor anomalies. Better classification may be obtained if the multi-image is preprocessed before classification, so as to reduce the adverse effects of image formation. In this paper, we discuss the overall impact on multi-spectral image classification when the retinex image enhancement algorithm is used to preprocess multi-spectral images. The retinex is a multi-purpose image enhancement algorithm that performs dynamic range compression, reduces the dependence on lighting conditions, and generally enhances apparent spatial resolution. The retinex has been successfully applied to the enhancement of many different types of grayscale and color images. We show in this paper that retinex preprocessing improves the spatial structure of multi-spectral images and thus provides better within-class variations than would otherwise be obtained without the preprocessing. For a series of multi-spectral images obtained with diffuse and direct lighting, we show that without retinex preprocessing the class spectral signatures vary substantially with the lighting conditions. Whereas multi-dimensional clustering without preprocessing produced one-class homogeneous regions, the classification on the preprocessed images produced multi-class non-homogeneous regions. This lack of homogeneity is explained by the interaction between different agronomic treatments applied to the regions: the preprocessed images are closer to ground truth. The principle advantage that the retinex offers is that for different lighting conditions classifications derived from the retinex preprocessed images look remarkably "similar", and thus more consistent, whereas classifications derived from the original images, without preprocessing, are much less similar.

Keywords: image classification, image enhancement, multi-spectral, retinex, dynamic range compression

1. INTRODUCTION

The analysis of remote sensed imagery obtained over agricultural regions can be used for the detection and discrimination of "stressed" and "non-stressed" vegetation; this is an issue of considerable importance to the agriculture industry. The terms "stressed" and "non-stressed" are used in a qualitative sense to designate the relative plant growth over different regions of a field. The differences in growth patterns can be due to several factors including different agronomic treatments. Various algorithms for the discrimination and detection of vegetation using remote sensed imagery exist in the literature. One way to characterize these algorithms is by the characteristics of the multi-dimensional space in which they operate. For example, many users of remote sensed imagery use spectral signatures to characterize and identify materials in multi-dimensional "spectral" space. The spectral signature of a material can be defined in the solar-reflective spectral region by its reflectance as a function of wavelength, measured at an appropriate spectral resolution. In other spectral regions, signatures of interest are temperature and emissivity (Thermal Infrared TIR) and surface roughness (radar).[1]

There are fundamental problems with the spectral signature approach that are well documented in the literature. First, all spectral signatures are unique to the sample and the environment in which they are obtained. Second, the ability to distinguish spectral signatures is often complicated by natural variability for a given material, spectral quantization of many remote-sensing systems, and modification of signatures by the atmosphere as a result of the image formation process.[1] Therefore, even though one may wish to apply different "labels" to differentiate vegetation

Further author information: (Send correspondence to B.T.)
B.T.: E-mail: bthompso@cs.wm.edu
Z.R.: E-mail: zrahman@cs.wm.edu
S.P.: E-mail: park@cs.wm.edu

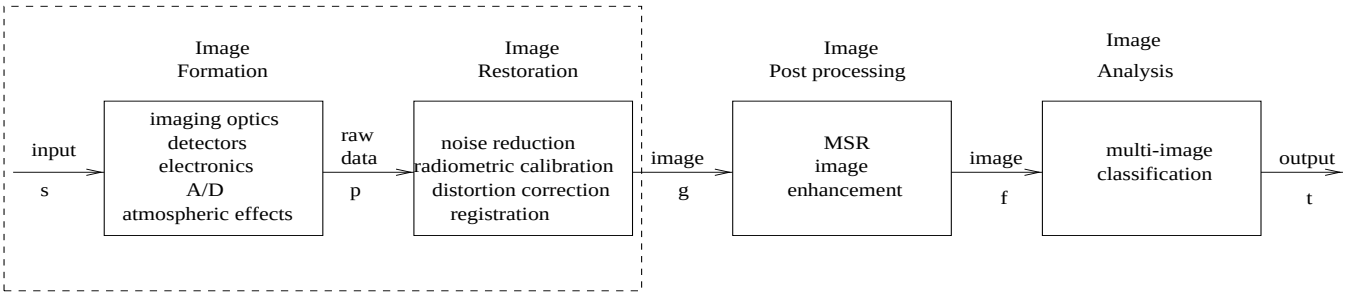

Figure 1. System Model

signatures, there is no guarantee that the signatures obtained by the remote sensing system will exhibit measurably different, or even recognizable, signatures.

In recent years, a considerable amount of ground-based (laboratory) data have been accumulated that describe spectral reflectance characteristics of soils and vegetation, without the problem of atmospheric complications. It is difficult, however, to duplicate natural reflectance measurements under laboratory conditions. The comparison between natural reflectance signatures and laboratory produced signatures, therefore, becomes even more complicated. Furthermore, the spectral signature of vegetation also changes over the seasonal life cycle of many plants, acquiring a "yellow" characteristic in senescence,* with a corresponding increase in the red region reflectance caused by a loss of photosynthetic chlorophyll.[1]

As an alternative to classification based on spectral signatures, multi-dimensional spectral space is transformed into a "feature" space prior to classification. In this way, information in the image is redistributed into a different and, depending on the application, more useful form. For example, transformations such as multi-spectral ratios of Near Infrared (NIR) to visible bands have been used to enhance reflectance differences between soils and vegetation and form "vegetation indices" that aid in classification. In this way, soil and other geological formations will exhibit similar ratios near 1, while vegetation will show a relatively larger ratio of 4 or more. Other common vegetation indices are the Normalized Difference Vegetation Index (NDVI), Soil-Adjusted Vegetation Index (SAVI), Transformed Vegetation Index (TVI), and the Perpendicular Vegetation Index (PVI).[1] The success of using these indices in the past has been affected by relatively few acquisition dates during a growing season, the paucity of ground truth data at the time of acquisition, and the lack of suitable methods to account for atmospheric effects on the radiance measured by the remote sensing device.[2]

Whether a particular classification algorithm uses spectral signatures or multi-spectral ratio indices to facilitate discrimination and detection of vegetation changes in an agricultural region, either technique requires good radiometric calibration of the image before analysis can be performed. Figure 1 illustrates the major steps in the image classification process. Radiometric calibration, a fundamental stage in this process, generally involves (1) sensor calibration: at-sensor radiance values obtained from quantized data during A/D conversion, (2) atmospheric correction: surface radiance values obtained from at-sensor radiance, and (3) solar and topographic correction: surface reflectance values obtained from surface radiance. Usually, detailed information about atmospheric conditions is not available for a given data set. However, parametric atmospheric correction methods can generally be used to compensate for atmospheric conditions. The success of multi-image classification in the analysis stage is based on the quality of these methods.

In this paper, we approach multi-image classification differently. Instead of using band ratios or absolute spectral signatures, we use "relative" signatures in the image to discriminate and detect vegetation changes. We compensate for the atmospheric effects on the multi-spectral images by applying the multi-scale retinex[3] (MSR) image enhancement algorithm to the multi-image, prior to image classification.

2. AGRONOMIC DATA

For our analysis we used remote sensed images of a cotton field in Texas acquired in the summer of 1997. We chose two multi-spectral images of the field taken on consecutive dates. The first image (acquired 08/14/97) has overcast

*Senescense is the physiological death of plants.

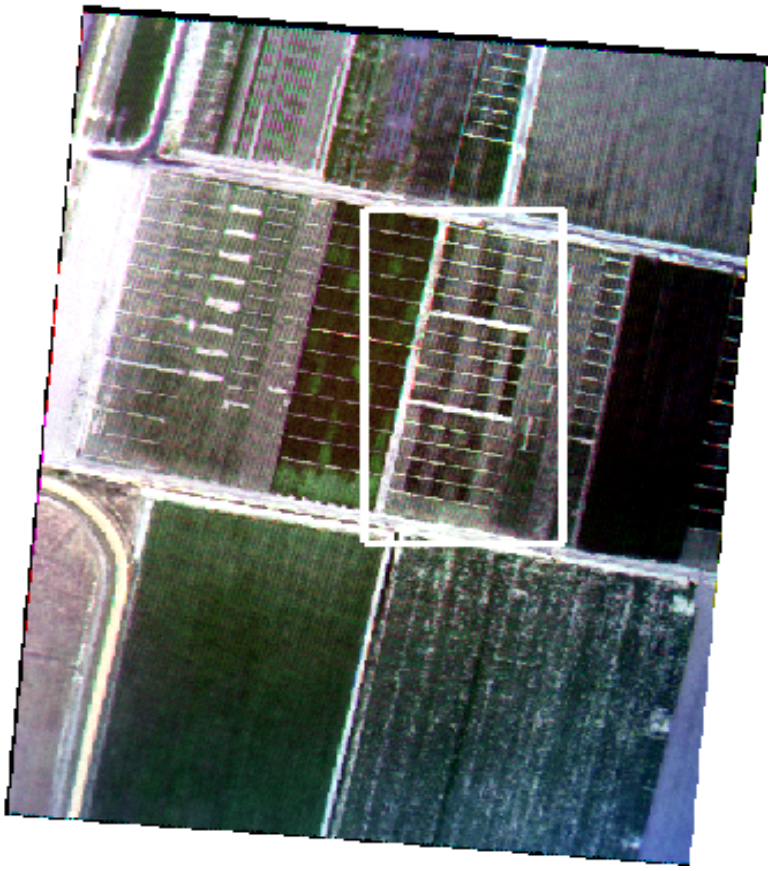

Figure 2. Test site captured on 08/14/97. The area of interest is highlighted within the rectangle.

sky, i.e. diffuse light, and the second (acquired 08/15/97) has almost clear sky, i.e. direct sunlight. The highlighted sub-image in Figure 2 is the area of interest for this experiment. We label the images of this area TXoa for date 08/14/97 and TXob for date 08/15/97. The cotton field was the site of a controlled experiment to study the effects on vegetation growth of different combinations of water and nitrogen treatment levels for a particular soil tillage type.[†] In all, 4 water treatment levels, 5 nitrogen treatment levels, and 2 soil tillage types were used. Figure 3 shows a schematic of the treatment experiments applied to the TXoa and TXob regions.

The field was divided into 120 blocks representing $4 \cdot 5 \cdot 2 = 40$ unique combinations of water, nitrogen, and tillage type. Each combination was repeated 3 times over the whole field. The 4 irrigation levels used were: 0.00, 0.25, 0.50 and 0.75 (fraction) of potential evapotranspiration (PET)[‡]. The 5 fertilizer nitrogen application levels were: 0, 20, 40, 60 and 80 lbs/acre Best Practice (BP)[§].

In theory, each of these 40 unique blocks represents a different "spectral class" and there are three samples of each class. However, classification results show that the number of actual spectral classes is fewer than 40. Moreover, the blocks are generally not homogeneous. That is, within each block there are *mixed* areas where the levels of water and/or nitrogen treatment are not uniform. In addition, the ground truth data was reliable for water treatment, but

[†]Tillage prepares the soil for growing crops. This preparation is traditionally accomplished by using a plow to cut and mix the soil.

[‡]Evapotranspiration (ET) is a measurement of the total amount of water needed to grow plants and crops. Since there are thousands of cultivated plants, the potential ET (PET) is a standard ET rate for general reference and use. The water requirements of specific crops and turf grasses can be calculated as a fraction of the PET. This "fraction" is called the crop coefficient (Kc) or turf coefficient (Tc)[4]

[§]Best Management Practices are farming practices that are designed to reduce nutrient contamination of surface and ground water. These practices are based on research results and field experiments and maybe as simple as following fertilizer recommendations and irrigation scheduling.[5]

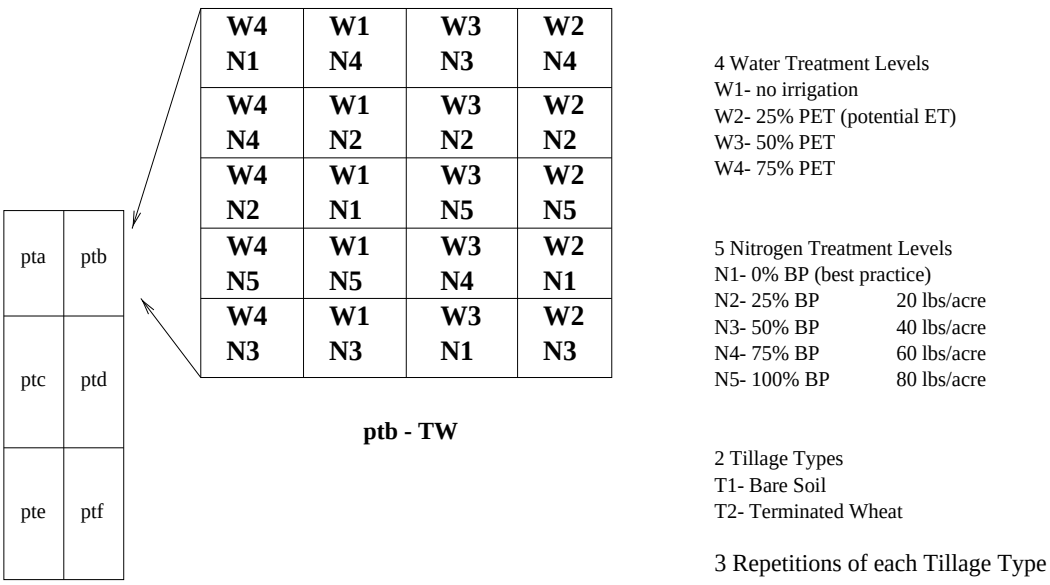

Figure 3. Agronomic treatments applied to the area of interest in Figure 2.

not for nitrogen treatment. The four-band multi-spectral images were acquired from an aircraft platform with an approximate nadir view, and calibrated to reflectance. The aircraft multi-spectral sensor band centers were at 486, 560, 685, and 840 nm.

3. IMAGE PREPROCESSING

3.1. The Multi-scale Retinex

For all (x, y) pixels in the multi-spectral image G, the multi-scale retinex (MSR)[6,7] can be compactly written as

$$F_j(x,y) = \sum_{n=1}^{N} W_n \cdot \{\log[G_j(x,y)] - \log[G_j(x,y) * H_n(x,y)]\} \tag{1}$$

where the subscript j represents the spectral bands, N is the number of spatial scales being used, and W_n are the weighting factors for the scales.[8,9,3] The $H_n(x,y)$ are the surround functions (convolution kernels) given by

$$H_n(x,y) = I_n \exp[-(x^2+y^2)/\sigma_n^2], \tag{2}$$

where the σ_n are spatial scale parameters that control the extent of the surround function. Smaller values of σ_n provide more dynamic range compression, and larger values provide more lightness/color constancy. The I_n are selected so that $\sum\sum H_n(x,y) = 1$. Each of the expressions within the summation represents a single-scale retinex (SSR).

The MSR combines the dynamic range compression of the small scale retinex with the tonal rendition of the large scale retinex to produce an output which encompasses both. Two fundamental issues in the application of the MSR are the following:

1. The MSR reduces dependency on lighting conditions/geometry caused by such conditions as obscured foregrounds, and poor lighting caused by defects in illumination due to atmospheric conditions or artificial illuminants.

2. As atmospheric conditions change, the MSR will produce results such that the restored image f in Figure 1 will look as much like the original scene s as possible, before image acquisition/digitization.

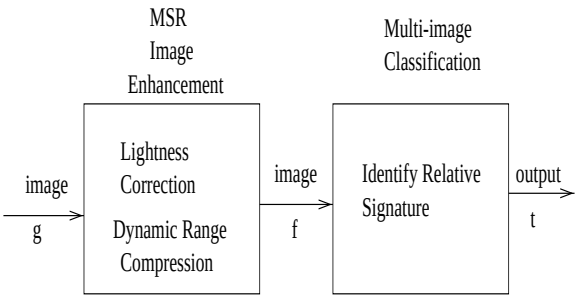

Figure 4. Post processing system model.

4. DISCUSSION

There were two primary motivations for this study: (a) to what extent can a conventional unsupervised classification algorithm yield "good" results when applied to the original images "as is" (i.e., with no preprocessing); and (b) if the multi-spectral images are preprocessed with the retinex algorithm and then the same conventional unsupervised classification algorithm applied, to what extent does that retinex processing influence the "goodness" of the result? This section summarizes the results of our initial experiments.

4.1. MSR Pre-classification Processing

The MSR was used to preprocess the multi-spectral image before it was used for classification. Figure 5 shows the results of the MSR algorithm applied to band 3 (685 nm) of the image in Figure 2. The left column shows the original images: TXoa and TXob, for the cloudy and clear day. The right column shows the MSR processed images: TXra and TXrb. In TXoa the band reflectance is uniformly very dark, because of the cloud cover on that day. The low contrast in this image creates a problem in obtaining spectral signatures that adequately discriminate agronomic variables. After the image is processed with the MSR, subtle patterns emerged that were not visible in the TXoa image. Specifically, the patterns represent the boundaries between the 20 different nitrogen and water treatment regions. The MSR also improved the TXob image, obtained on the clear day. One of the primary results from the application of the MSR is that the processed images, TXra and TXrb, are more "similar" to each other in brightness, contrast and detail than the original images, TXoa and TXob.

The MSR processed images display far more visual information than is evident in the unprocessed images. Even though radiometric calibration is not preserved by the MSR, we conclude that it can be used as an auxiliary tool for the visualization of spatial patterns in dark regions, as is demonstrated herein. Visual information in darker regions that may not be detected with linear representations which preserve radiometry will "pop out" with a clarity limited only to the dynamic range of the sensor and any intervening digitalization scheme used prior to the MSR. For this experiment, we have not yet conducted extensive performance comparison of the MSR with other image enhancement algorithms such as histogram equalization, gamma correction, and point logarithmic nonlinearity. However, we expect to find that those image enhancement algorithms are not appropriate for use in preprocessing multi-spectral images for remote sensing applications where atmospheric conditions are the major contributor to data inaccuracy.

4.2. Multi-image Classification

The literature is rich with both supervised and unsupervised methods for classifying remote sensed multi-spectral images. These methods include spatial/spectral discriminant functions, e.g., the Maximum Likelihood, and spectral specific methods, e.g., linear mixing models that require some a priori knowledge such as ground truth maps or ground samples. Whereas, supervised classification requires training sets to teach the classifier to recognize certain specific features in the image, unsupervised methods require little or no training data and attempt to discover the underlying patterns in multi-dimensional space by using techniques such as gradient descent. In this experiment, we have limited a priori information available about the field being analyzed. The a priori information was used to verify the accuracy of the classes obtained using unsupervised classification.

We used vector quantization (VQ) to perform unsupervised classification on the multi-spectral image. The only user specified parameter is the number of classes K. The primary goal was to study and compare the effects of MSR

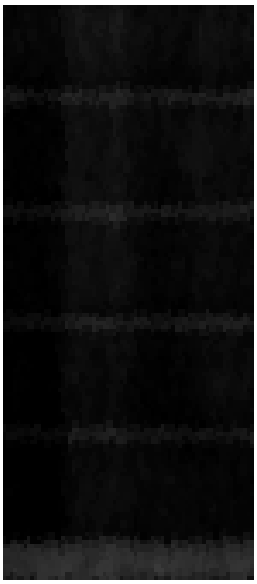

08/14/97 TXoa

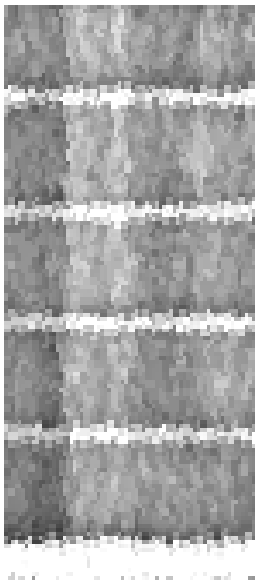

08/14/97 TXra

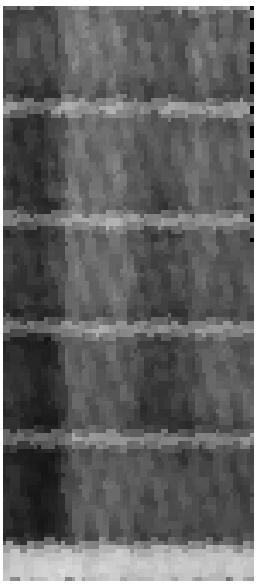

08/15/97 TXob

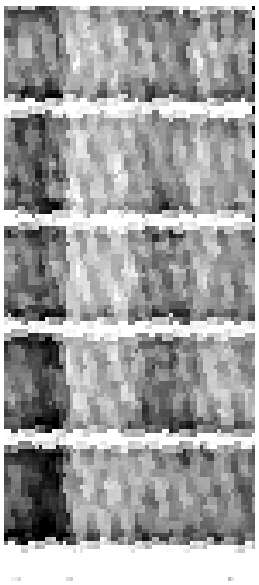

08/15/97 TXrb

Figure 5. TX Images– Original and retinex processed images.

Table 1. List of constants used to process the TXoa and TXob images with the MSR

Constant	σ_1	σ_2	σ_3	σ_4	Gain	Offset
Value	2	5	20	200	180	0.57

preprocessing on the classification results. The same classification algorithm was applied to both of the *original* four-band images TXoa, TXob and both of the *MSR* four-band images TXra, TXrb. For all four images, we systematically experimented with K to see how the number of classes affects the overall classification results.

To cluster the images we used VQ along with a splitting method to define the spectral signatures. The method starts with a one-level quantizer (i.e., the centroid of the entire training set). Next, the one-level quantizer vector is split into two vectors obtained by perturbing the one-level quantizer. The 2-level quantizer is then applied to the training set. The two 2-level quantizer vectors are then split into four vectors and a 4-level quantizer is applied to the training set. The splitting is continued in this manner until K code vectors are generated. This method assumes that K is a power of two. If K is not a power of two, then in the last step, instead of generating two new code vectors from each of the code vectors of the quantizer designed previously, we can perturb as many code vectors as necessary to obtain the desired number of code vectors.[10] As in most classification methods, the performance depends on the quality of the set of spectral means used to discriminate classes in the image. For this analysis, we did not focus on methods to obtain spectral means, but compared the relative accuracy of the spectral means obtained by the VQ to signatures derived from the training areas defined by the schematic map of Figure 3.

5. CLASSIFICATION RESULTS

Figures 6 and 7 show the classification results for the original and MSR preprocessed images. To examine the accuracy of our results we compare these results to the schematic plot of the proposed treatment of water and nitrogen for the cotton field shown in Figure 3. To facilitate analysis, the figures are annotated with a grid that provides an approximate separation boundary between each treatment level block.

Our classification results were very encouraging for a number of classes, from as few as $K = 4$—(i.e., 4 water treatment levels), to as many as $K = 40$—(i.e., 4 water treatment levels $\times$ 5 nitrogen treatment levels $\times$ 2 tillage types). For the case $K = 4$, we were interested in determining how well the four water treatment levels could be discriminated in the image. In the case $K = 8$, we were interesting in discriminating the four water treatment levels for each tillage type. From our results we did not see any major differences between the different tillage types in terms of classification results. That is to say, we could not resolve two different classes of each water treatment type. The primary effect of the case $K = 8$ was that we were able to see more clearly the water-nitrogen iterations.

Generally, for all four images we were able to see very clearly the "block" treatment structure that is present. There are differences in the results, however, depending on whether the lighting was diffuse or direct and depending on whether or not retinex preprocessing was used. The left column of Figures 6 and 7 show that without MSR preprocessing the blocks tend to be classified as homogeneous (one class); the right column of Figures 6 and 7 show that with MSR preprocessing the blocks tend to be classified as more non-homogeneous (multi-class). Comparison of the classification results for TXoa, TXob (original images) and TXra, TXrb (MSR processed images), show considerable variation in classes for the unprocessed images as the atmospheric and lighting conditions vary, but slight or no variations for the MSR processed images.

Because consistent classification results are achieved regardless of the atmospheric conditions, we can argue empirically that MSR preprocessing tends to produce "spectral signature images". Note that classification consistency in this experiment is really a measure of the resiliency of the classification process to changes in the process that affect the formation of the multi-spectral image. In other words, classification consistency is really a measure of how well we can classify the multi-spectral image given that the atmospheric conditions have changed substantially from day to day. To illustrate classification consistency, in Table 2 we show the mean spectral reflectance measurements for the original and MSR preprocessed images for each class. From this table we see that the spectral signatures for the MSR preprocessed images for each day are more similar than the signatures for the original images.

Initially, we expected to see one different class for each column in the field representing a different water treatment level and not the multi-class variations that are shown in Figures 6 and 7. However, because the nitrogen and water

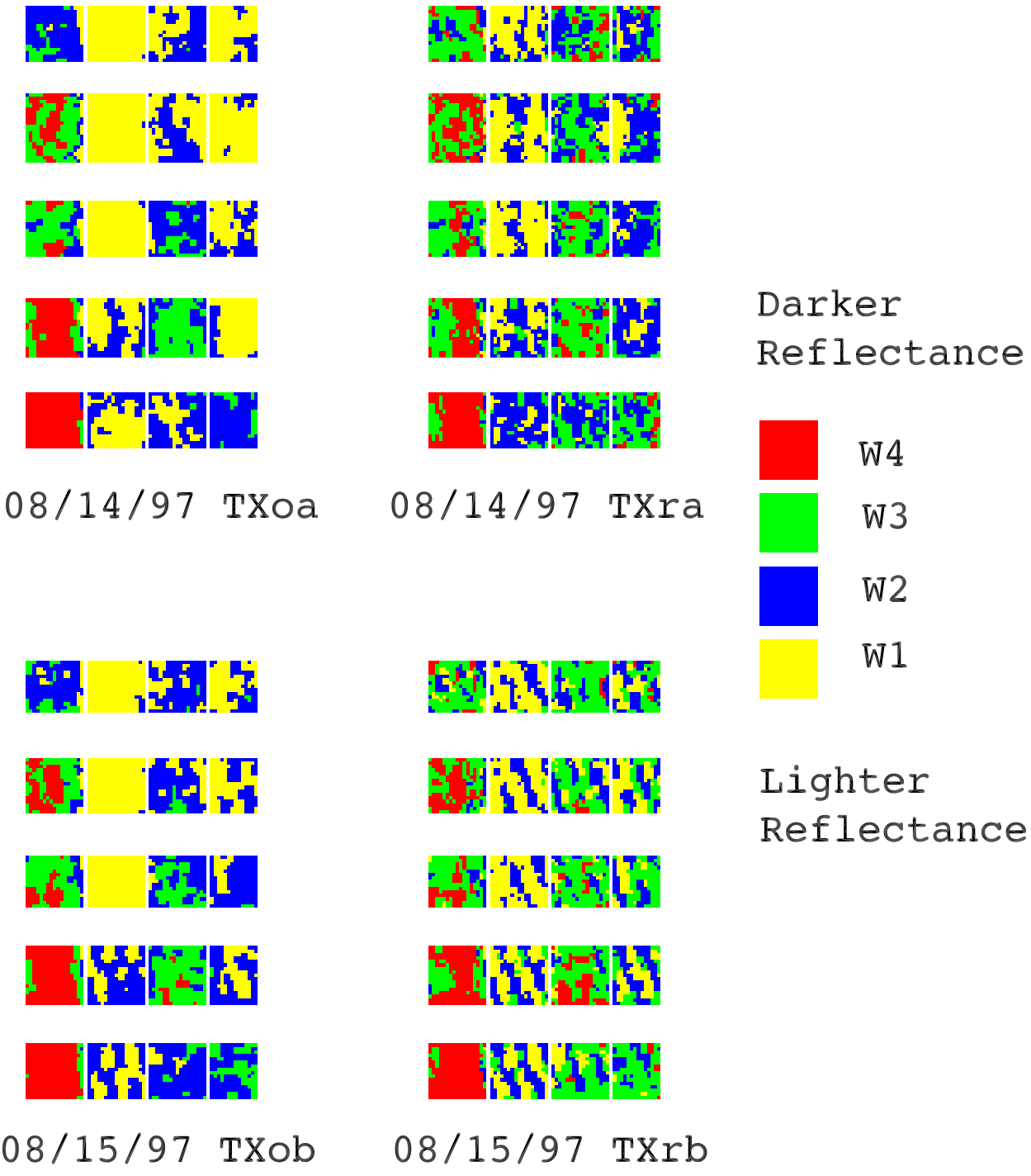

Figure 6. Classification Results: 4 Classes

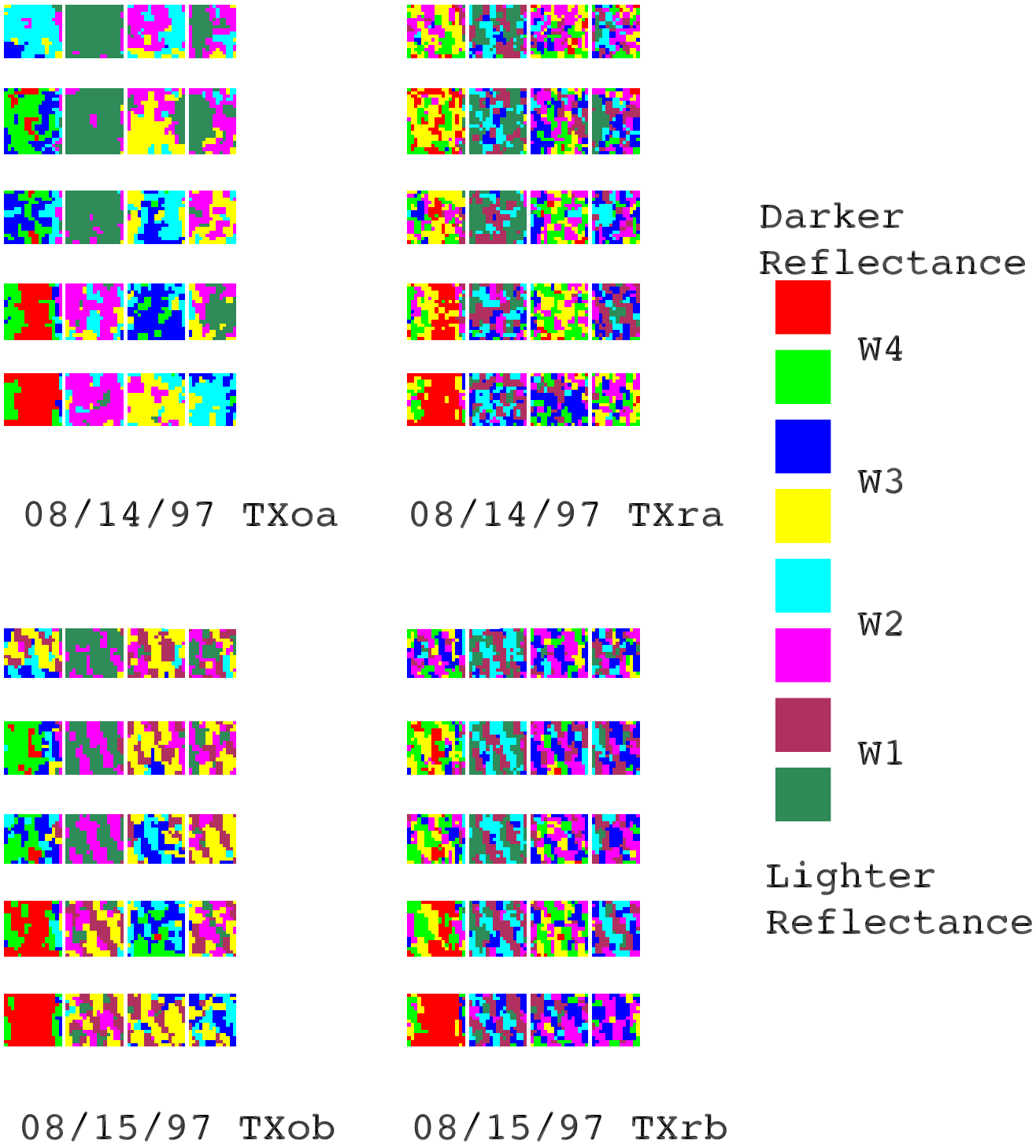

Figure 7. Classification Results: 8 Classes

Table 2. Mean spectral reflectance measurements for each class.

Class	Wavelength (nm)							
	486	560	685	840	486	560	685	840
	08/14/97 diffuse				08/14/97 MSR			
W4	55	49	33	102	140	138	123	161
W3	58	52	38	93	146	145	139	155
W2	60	54	41	104	151	148	151	146
W1	63	58	45	90	158	157	167	144
	08/15/97 direct				08/15/97 MSR			
W4	115	113	66	201	124	119	92	156
W3	127	128	83	195	143	140	126	152
W2	136	138	97	190	146	148	159	149
W1	148	149	106	190	169	167	173	147

Table 3. Mean spectral reflectance measurements for each column in Plotb of Figure 3.

Column	Wavelength (nm)								Class
	486	560	685	840	486	560	685	840	
	08/14/97 diffuse				08/14/97 MSR				
1	54.83	50.68	33.49	103.65	140.46	141.93	125.12	162.60	W4
2	60.37	54.88	41.54	91.22	154.25	153.09	156.12	145.28	W1
3	56.77	52.15	36.85	94.85	143.66	143.80	134.99	153.09	W3
4	58.29	53.42	39.12	92.49	148.19	147.92	144.54	150.00	W2
	08/15/97 direct				08/15/97 MSR				
1	102.07	104.53	61.38	176.28	128.47	127.800	101.82	156.43	W4
2	124.47	126.46	91.42	162.21	157.97	157.38	164.08	146.14	W1
3	112.83	115.05	76.03	165.88	141.24	140.29	130.38	151.37	W3
4	117.06	120.30	83.67	162.03	147.88	147.31	145.53	149.41	W2

treatment affect the vegetation growth jointly, it would be a mistake to consider the two treatments independently. For example, the effect of applying water treatment level 4 and nitrogen level 3 may be the same as applying water treatment level 3 and nitrogen level 5. Therefore the original assumption that there are 40 distinct classes is, of course, not valid. In further study, we realized that what we are actually discriminating is the change in reflectance due to different nitrogen effects *and* water treatment, i.e., joint effects. In Table 2 we see that reflectance generally increased with water stress for all water levels in the 486, 560, and 685 nm wavelength, but decreased in the (NIR) 840 nm range. This increase in reflectance effect has been reported elsewhere as the effect water stress has on diffusive resistance and plant metabolism in general.[11] However, the increase was affected by the nitrogen treatments applied. These same measurements all showed a clear nitrogen and water stress interaction.[¶] Thus water treatment labels for each class were identified as W4 for the darkest spectral reflectance in the 486, 560, and 685 nm range and W1 for the lightest reflectance in that same range.

To identify the water treatment levels, we matched the mean spectral reflectance measurements of each column in Table 3 for the original and MSR processed images shown in Figure 3 with the mean spectral reflectance for each class shown in Table 2. From this analysis we were able to conclude that the mean spectral reflectance for each column matched the correct mean spectral reflectance for each class. Although the magnitude of the results may be different for other tillage types, the results presented here should prove useful for determining the amount of information that can be expected from particular agronomic variable interactions for given atmospheric conditions.

[¶]This merits a re-examination of the data, which is the subject for another paper.

6. CONCLUSIONS

Spectral signatures alone do not provide adequate classification of a scene, especially if the atmospheric or lighting effects have severely affected the multi-image components.[1] This is evident if we compare the classification results before and after MSR preprocessing. Without additional ground truth, or results from other classification studies, it is difficult to state with any confidence whether the classifications obtained with the preprocessed images are "better" in some absolute sense than the classifications obtained from the original images. We can state, however, that the classifications from the MSR preprocessed images for the two different lighting and atmospheric conditions are remarkably "similar" both visually, and in terms of the mean spectral reflectance of a class. We speculate that this occurs because the MSR preprocessing is minimizing the effects of the atmospheric conditions on the multi-spectral image, leading to consistent classifications from consistent data.

To summarize, we conclude that conventional unsupervised classification can be applied to this significant problem of detection and discrimination of stressed and unstressed vegetation. Although classification results from both the original and the MSR preprocessed images are encouraging, the MSR preprocessed images are more robust to changes in atmospheric and lighting conditions. We need to conduct additional experiments to test the validity of our speculation that MSR preprocessed multi-image classification is more robust in the presence of atmospheric and lighting changes. In addition, we need to substantiate our conjecture that other image enhancement algorithms do not have the same "beneficial" effect on the classifications. A color version of the figures in this paper is available at http://dragon.larc.nasa.gov/viplab/retinex/background/pubabs/spie3716-1999.html.

ACKNOWLEDGMENTS

The authors would like to thank Dr. Pamela Blake, Dr. Joan Hayashi, and Jim Sweet of GDE Systems, Inc for the use of the multi-spectral images and ground truth data. This research was supported by the Virginia Space Grant Consortium (VSGC), NASA Graduate Student Researchers Program (GSRP), and NASA Langley Research Center Cooperative Agreement NCC-1-258.

REFERENCES

1. R. A. Schowengerdt, *Remote Sensing: Models and Methods for Image Processing*, Academic Press, 1997.
2. R. Jackson, P. Slater, and P. J. Pinter, "Discrimination of growth and water stress in wheat by various vegetation indices through clear and turbid atmospheres," *Remote Sensing of Environment* , 1983.
3. D. J. Jobson, Z. Rahman, and G. A. Woodell, "A multiscale retinex for bridging the gap between color images and the human observation of scenes," *IEEE Transactions on Image Processing* , 1997.
4. T. A. E. Service, *PET Documentation*, Texas Evapotranspiration Web Site: http://www.agen.tamu.edu/pet.
5. N. E. Derby, R. E. Knighton, and D. D. Steele, *Temporal and Spatial Distribution of Nitrate Nitrogen Under Best Management Practices*, North Dakota State University, Department of Soil Science, 1994.
6. E. H. Land, "The retinex theory of color vision," *Scientific American* , pp. 108–129, December 1977.
7. M. Olshaker, *The Instant Image: Edwin Land and the Polaroid Experience*, Stein and Day, Scarborough House, Briarcliff Manor, N.Y., 1978.
8. Z. Rahman, D. J. Jobson, and G. A. Woodell, "Multiscale retinex for color image enhancement," *International Conference on Image Processing ICIP'96* , 1996.
9. D. J. Jobson, Z. Rahman, and G. A. Woodell, "Properties and performance of a center/surround retinex," *IEEE Transactions on Image Processing* , 1997.
10. K. Sayood, *Introduction to Data Compression*, Morgan-Kaufmann, 1995.
11. J. Schepers, T. Blackmer, W. Wilhelm, and M. Resende, "Transmittance and reflectance measurements of corn leaves from plants with different nitrogen and water supply," *J. Plant Physiol* (148), pp. 523–529, 1996.